Hybrid Particle-Field Simulations of Polymer Nanocomposites

Scott W. Sides,[1] Bumjoon J. Kim,[2] Edward J. Kramer,[2] and Glenn H. Fredrickson[2]

[1]*Tech-X Corporation, Boulder, Colorado 80305, USA*

[2]*Departments of Chemical Engineering and Materials and Materials Research Laboratory, University of California, Santa Barbara, California 93106, USA*

(Received 18 April 2006; published 27 June 2006)

We present a theoretical framework and computer simulation methodology for investigating the equilibrium structure and properties of mesostructured polymeric fluids with embedded colloids or nanoparticles. The method is based on a field-theoretic description of the fluid in which particle coordinates and chemical potential field variables are simultaneously updated. The fluid model can contain polymers of arbitrary chemical and architectural complexity, along with particles of all shapes, sizes, and surface treatments. Simulation results are compared with experiments conducted on polystyrene (PS)-functionalized Au nanoparticles in a PS-P2VP diblock copolymer melt.

DOI: 10.1103/PhysRevLett.96.250601 PACS numbers: 05.10.−a, 02.70.−c, 82.20.Wt

The fields of colloid science and soft material nanoscience rely on the ability to control the self-assembly of solid particles that are suspended in complex fluid media. Surfactants, dispersants, and other species are commonly added to the fluid to enhance stability and to improve the uniformity of a particle dispersion. A more recent theme that has emerged with the increasing availability of nanosized inorganic particles is the use of mesostructured fluids to sequester and arrange particles into useful inhomogeneous assemblies.

Recent studies have used a variety of techniques to investigate the effects of particles dispersed in complex fluids such as block copolymers. These methods include modified strong-segregation theories [1], Monte Carlo (MC) [2,3] and molecular dynamics [4] simulations, as well as a method that couples a phenomenological Cahn-Hilliard picture for the fluid with Brownian dynamics for the particles [5,6]. While some progress has been made with these techniques, reliable simulation tools for studying mesostructured fluid or particle composites are lacking. The length and time scales involved for realistic copolymer systems are normally beyond the realm of atomistic simulations, and no reliable analytical tools are available for addressing the broad spectrum of inhomogeneous structures that can form in such systems.

Self-consistent field theory (SCFT) is a powerful method for studying the complex morphologies of multicomponent block copolymers and blends [7–9]. SCFT is based on a saddle-point (mean-field) approximation to a field-theoretic description of a polymeric fluid. The theory captures architectural details of the polymers and can be applied for both unit cell and large calculations [10–13].

A recent numerical scheme by Thompson, Balazs, and co-workers has addressed a class of nanoparticle dispersion problems by coupling SCFT for inhomogeneous polymers with a density functional theory (DFT) for hard spheres to create an approximate energy functional whose extrema correspond to mean-field solutions [14–16]. While quite promising, the SCFT-DFT approach is difficult to extend beyond classes of systems for which reliable density functionals are available, and it is not apparent how to go beyond the mean-field approximation in the treatment of the polymer fluid fields and how they influence nanoparticle morphologies.

In the present Letter we introduce a new simulation methodology for mesostructured polymeric fluids with embedded particles that in principle does not suffer from these limitations. As in the SCFT-DFT approach, our method describes the fluid structure in a field-theoretic context, although we are not restricted to the mean-field approximation implied by SCFT. Unlike the SCFT-DFT method, we explicitly retain the particle coordinates as degrees of freedom, rather than impose a DFT approximation. In this regard, our hybrid particle-field (HPF) description is reminiscent of the Car-Parrinello [17] technique for conducting *ab initio* molecular dynamics.

The HPF method is based on the use of ''cavity'' functions to exclude the fluid components from the interior of solid particles. For example, in the case of spherical particles, a spherically symmetric cavity function $h(r)$ can be defined, which is a continuous differentiable function that varies from 1 at $r = 0$ (inside the particle) to 0 at $r \to \infty$ (outside the particle). A useful choice is a monotonically decreasing function $h(r)$ with a slow scale R_p defining the particle radius and a fast scale ξ defining the width of the particle-fluid interface. For a set of m *nonoverlapping* particle positions $\mathbf{r}^m = (\mathbf{r}_1, \ldots, \mathbf{r}_m)$, the function

$$\rho(\mathbf{r}; \mathbf{r}^m) = \rho_0 \left[1 - \sum_{j=1}^{m} h(|\mathbf{r} - \mathbf{r}_j|) \right] \tag{1}$$

represents a density field for the complex fluid species surrounding the particles. This field vanishes at positions $\mathbf{r}$ inside a particle and is constant at ρ_0 for $\mathbf{r}$ outside a particle. As is typical in a mesoscopic description, we shall

assume the fluid to be incompressible with a density given by Eq. (1).

A field theory for the polymeric fluid can be formulated in the usual way by applying Hubbard-Stratonovich (HS) transformations to decouple interactions between different macromolecular species. These HS transforms introduce auxiliary chemical potential fields $w(\mathbf{r})$, which become the relevant fluctuating degrees of freedom defining the fluid; the conformational and translational degrees of freedom can be explicitly integrated out. For example, in the familiar Edwards model of flexible homopolymers dissolved in a good solvent [18], this procedure leads to a field theory description corresponding to a canonical ensemble of n polymers in a volume V ($k_BT = \beta^{-1} = 1$), with an effective "fluid" Hamiltonian

$$\mathcal{Z}(n, V, T) = \int \mathcal{D}w \exp(-H_f[w]), \tag{2}$$

$$H_f[w] = (1/2u_0) \int d\mathbf{r} w^2 - n \ln Q[iw]. \tag{3}$$

Here, $u_0 > 0$ is the excluded volume parameter between polymer segments and $Q[iw]$ is a nonlocal functional that represents the partition function of a *single* polymer in a purely imaginary potential $iw(\mathbf{r})$. $Q[iw]$ can be computed for prescribed $w(\mathbf{r})$ from the solution of a complex diffusion equation that can be viewed as a Feynman-Kac formula for the path integral defining $Q[iw]$. Similar field-theoretic models can be constructed for compressible and incompressible models of polymer solutions and melts with arbitrary numbers of components and polymer architectures [13].

The coupling between the w field variables, which define the fluid structure, and the particle coordinates arises through the cavity functions discussed above. In performing the HS transformation for an incompressible fluid with embedded particles, the exclusion of polymer from the interior of the particles can be accounted for by including the local constraint

$$\prod_{\mathbf{r}} \delta(\hat{\rho}(\mathbf{r}) - \rho(\mathbf{r}; \mathbf{r}^m)) \tag{4}$$

inside the configurational integral. Here $\hat{\rho}(\mathbf{r})$ is a "microscopic" density operator composed as a sum of delta functions centered on the positions of all segments (and solvents if present) that compose the fluid. Upon giving this delta functional an exponential representation, we find a linear coupling term in the Hamiltonian of the field theory given by

$$H_{pf1}(\mathbf{r}^m; [w_+]) = -i \int d\mathbf{r} \rho(\mathbf{r}; \mathbf{r}^m) w_+(\mathbf{r}). \tag{5}$$

The "pressure" field $w_+(\mathbf{r})$ is a fluctuating chemical potential that enforces the constraint (4).

In a multicomponent fluid model, additional fluctuating "exchangelike" chemical potential fields will serve to define the compositional structure of the fluid. For a two-component fluid (A and B), a tendency for enrichment of component A at the particle surfaces can be incorporated through a microscopic interaction term ($\lambda > 0$ for enrichment of A)

$$H_{pf2} = -\lambda \int d\mathbf{r} \Big[\sum_j h(|\mathbf{r} - \mathbf{r}_j|) \Big] [\hat{\rho}_A(\mathbf{r}) - \hat{\rho}_B(\mathbf{r})]. \tag{6}$$

Tracing this contribution through the HS transformation produces a linear shift $w_-(\mathbf{r}) \rightarrow w_-(\mathbf{r}) - \lambda \sum_j h(|\mathbf{r} - \mathbf{r}_j|)$ in the exchange potential w_- conjugate to $\hat{\rho}_A - \hat{\rho}_B$. Equation (6) can thus be reexpressed as a hybrid functional $H_{pf2}(\mathbf{r}^m; [w_-])$. Besides the fluid and particle-fluid contributions to the Hamiltonian, we can also include direct particle-particle interaction terms $H_{pp}(\mathbf{r}^m)$, e.g., pair interactions, that can be used to prevent particle overlaps. Combining contributions H_f, H_{pf1}, H_{pf2}, and H_{pp} yields a total effective Hamiltonian $H(\mathbf{r}^m; [w_\pm])$ for the HPF model.

For the purpose of numerical simulations, a pseudo-spectral approach, e.g., with a plane wave basis, has been shown to be highly efficient for evaluating the Hamiltonian H_f and the forces $\delta H_f / \delta w$ of a polymer field theory [19]. A similar strategy is effective here wherein a uniform collocation grid is maintained throughout the simulation cell, even in the particle interiors. Particle-field interaction terms in H, such as Eq. (5), can be efficiently evaluated on the grid by using a fast-Fourier-transform (FFT)-inverse FFT pair to evaluate the convolution integral and then summing over the grid points coinciding with the instantaneous particle centers. Using M ($\gg m$) grid points, a term like H_{pf1} can thus be evaluated in $O(M \log M)$ operations.

To sample the particle configurations, a Brownian dynamics (BD) or force-bias MC scheme is attractive because forces on all the particles can be computed in a single sweep of the grid, which is necessary anyway to update the fluid w fields. The force on particle j arising, e.g., by the coupling (5) can be written

$$\mathbf{F}_j \equiv -\frac{\partial H_{pf1}}{\partial \mathbf{r}_j} = -i\rho_0 \int d\mathbf{r} \mathbf{g}(\mathbf{r}_j - \mathbf{r}) w_+(\mathbf{r}), \tag{7}$$

where $\mathbf{g}(\mathbf{r}) \equiv \frac{1}{r} \frac{dh(r)}{dr} \mathbf{r}$ is a vector "virial" function. Equation (7), however, is again a convolution integral that can be evaluated by an FFT-inverse FFT pair. The forces on *all* the particles can thus be evaluated simultaneously.

To sample fluid field configurations, there are several options, the simplest being to relax the fields quasistatically to the saddle-point configuration satisfying $\delta H / \delta w_\pm = 0$ consistent with a given particle configuration $\mathbf{r}^m$. This amounts to a mean field or SCFT treatment of the fluid variables and circumvents the "sign problem" of sampling a nonpositive definite weight $\exp(-H)$ because the saddle-

point pressure field w_+ is purely imaginary and so H remains real for all particle configurations. Alternatively, without invoking any approximations, we could employ complex Langevin sampling for both particle and field variables [20,21].

In the present Letter we apply the HPF method to examine a model composite of hard sphere nanoparticles with molten diblock copolymers. We use a steepest descent algorithm to relax the polymer fields to their mean-field solution, as described in Ref. [22]. For updating particle positions, a BD algorithm can be applied [23]:

$$\Delta \mathbf{r}_j = \beta D \Delta t \mathbf{F}_j + \mathbf{R}_j, \tag{8}$$

where $\Delta \mathbf{r}_j$ is the displacement of particle j in a time step Δt, D is the diffusion constant in the absence of particle-particle interactions, and $\mathbf{R}_j$ is a Gaussian random variable. This dynamics scheme, which neglects hydrodynamic interactions, is simply a means of attaining equilibrium configurations. For this initial study, a simpler deterministic version of Eq. (8) is applied in which we set $\mathbf{R}_j = 0$ and choose $\beta D \Delta t$ such that the average particle displacement is $0.25 R_g$, where R_g is the radius of gyration of an unperturbed copolymer chain. This choice was found to result in reasonably rapid relaxation down the free energy landscape, while restricting large particle displacements that would require longer calculations to solve the fluid SCFT equations. To update the particle configuration at time step n, $\mathbf{r}_n^m$, to a configuration at time step $n+1$, $\mathbf{r}_{n+1}^m$, the full algorithm is as follows: (i) for $\mathbf{r}_n^m$, numerically solve the SCFT equations ($\sim$10–100 iterations of steps 2–5 in Ref. [22]); (ii) calculate $\mathbf{F_j}$ and $\Delta \mathbf{r}_j$ for each particle j using Eqs. (7) and (8); (iii) set $\mathbf{r}_{n+1}^m = \mathbf{r}_n^m + \Delta \mathbf{r}^m$, where $\Delta \mathbf{r}^m = (\Delta \mathbf{r}_1, \ldots, \Delta \mathbf{r}_m)$, and explicitly reject moves that cause particle-particle overlaps; (iv) return to step (i) and repeat until the polymer morphology stabilizes.

Experimental.—As templates for organizing nanoparticles two poly(styrene-b-2vinylpyridine) (PS-b-P2VP) diblock copolymers were used: a lamellar forming (LAM) copolymer with total molecular weight $M_n = 114$ kg/mol and PS volume fraction $f_{\mathrm{PS}} = 0.50$ and a cylinder forming (HEX) copolymer with $M_n = 61$ kg/mol and $f_{\mathrm{PS}} = 0.23$, both from Polymer Source, Inc. thiol terminated PS (PS-SH) was synthesized by living anionic polymerization in benzene at 30 °C [24] resulting in an M_n of 1.5 kg/mol and a polydispersity index of 1.1. PS coated Au particles were synthesized using the short PS-SH chains as stabilizing ligands via a two-phase (toluene and water) method [25]. The diameter of the Au core of these particles was 2.5 ± 0.7 nm and the densely packed PS-SH on the Au surface resulted in a PS shell 3 nm thick [26]. Films of mixtures of PS(Au) and PS-b-P2VP on an epoxy substrate were prepared by slowly casting from solutions in tetrahydrofuran, a solvent that is preferential for PS [24]. After drying and staining the P2VP domains with I_2 the films were microtomed into 25 to 40 nm thick slices for observation by transmission electron microscopy (TEM). The PS-shell thickness was estimated from the surface area of the Au cores (from TEM) and the weight fraction of PS-SH ligands on the Au (from thermal gravimetric analysis) [26].

Results of two-dimensional simulations with the HPF algorithm conducted on a 72×80 lattice are shown in Figs. 1 and 2 (copied in each direction to emphasize ordering) and compared to TEM images showing the spatial arrangement of (PS)-functionalized Au particles in a phase-separated melt of PS-P2VP diblock copolymers. The values of R_p, ξ, and λ in the simulations were chosen by matching the size and wetting characteristics of the Au-core/PS-shell nanoparticles. An average of 5×10^5 field updates were used to obtain the two figures. The experimental TEM data in Fig. 1 shows the PS (light) and P2VP (dark) domains for the $f_{\mathrm{PS}} = 0.5$ PS-P2VP diblock. The PS chains grafted to the Au-particle surfaces cause a net attraction between the nanoparticles (dark spots in TEM images) and the PS domains of the copolymer. At low nanoparticle densities, the Au particles are segregated to the lamellar domains. As the nanoparticle density increases, the PS lamellae become increasingly swollen

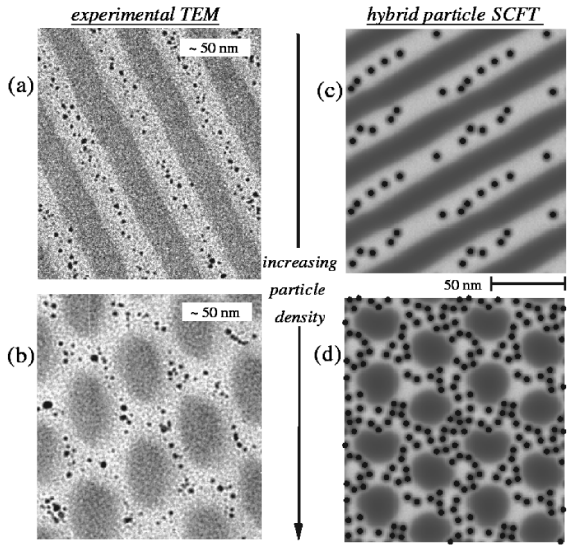

FIG. 1. TEM images of $f_{\mathrm{PS}} = 0.50$ PS-P2VP diblock nanocomposite containing (PS)-functionalized Au particles with particle volume fraction (a) = 0.10 and (b) = 0.35. Total particle size including the PS shell is 2.6 times that of the Au cores seen as black dots in the TEM images. HPF simulation results (right column) show monomer volume fractions representing PS (light), P2VP (dark), particles (black). Simulation parameters: $f_{\mathrm{PS}} = 0.5$, Flory parameter (χ) for PS-P2VP diblock $\chi = 0.16$, $\lambda = 0.16$, and particle area fraction (c) = 0.04 and (d) = 0.18. The particle configurations shown are representative of those obtained based on several independent runs for a given nanoparticle density. Note: The black circles in the SCFT simulations denote nanoparticle regions where $\rho/\rho_0 \leq 0.5$ and therefore represent not only the Au nanoparticle cores but also a significant portion of the surrounding PS shell.

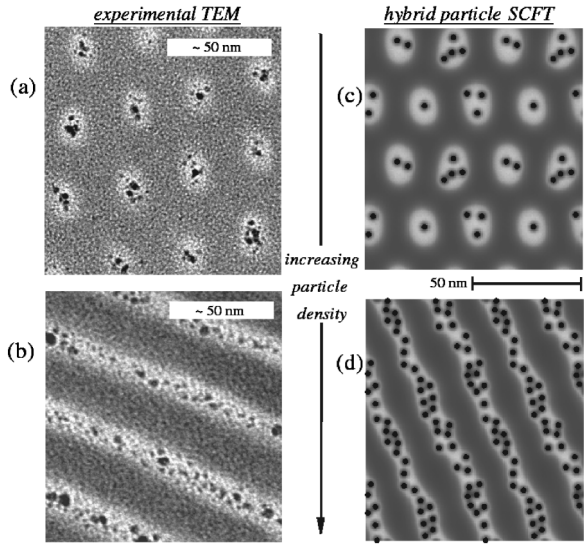

FIG. 2. TEM images of $f_{PS} = 0.23$ PS-P2VP diblock nanocomposite containing (PS)-functionalized Au particles with particle volume fractions (a) = 0.05 and (b) = 0.2. HPF simulation results shown in the right-hand column. Simulation parameters: $f_{PS} = 0.3$, $\chi = 0.18$, $\lambda = 0.16$, particle area fraction (c) = 0.03 and (d) = 0.12.

with particles and distorted. Eventually, the copolymer morphology is transformed into an arrangement of hexagonally packed cylinders at sufficiently high particle densities. The hybrid SCFT simulations in Fig. 1 show excellent qualitative agreement with experiment and confirm the particle-induced transition from LAM to HEX domains. The simulations in Fig. 2 show similar agreement to experimental data for the $f_{PS} = 0.23$ PS-P2VP diblock that displays a transition from the HEX to LAM phases upon increasing Au-particle density. In both cases, the hybrid SCFT results underestimate the particle density at the morphological transitions. Beyond the experimental uncertainty in determining the particle density at the transitions, we emphasize that the simulations were conducted in two dimensions. We surmise that future work on larger, 3D simulations will show improved quantitative agreement with experiment.

In summary, we have developed an efficient new simulation methodology for studying polymer nanocomposites. Our HPF algorithm combines the power of numerical SCFT methods for analyzing complex polymer morphologies with the flexibility of a particle-based simulation that is able to include particles with a variety of shapes, interactions, and surface treatments in a straightforward way. We emphasize that the HPF framework is easily extended to polymers and copolymers of virtually any architecture and to multicomponent mixtures of such molecules and with solvents. Future work will include extending the force algorithm to compute torques on nonspherical particles, implementing complex Langevin sampling of particles and fields to relax the mean-field approximation, and devising update algorithms with more realistic particle and fluid dynamics.

This work was supported in part by the MRSEC program of the NSF under Grant No. DMR05-20415 and by Tech-X Corporation.

[1] J. U. Kim and B. O'Shaughnessy, Phys. Rev. Lett. **89**, 238301 (2002).
[2] Q. Wang, P. F. Nealy, and J. J. de Pablo, J. Chem. Phys. **118**, 11 278 (2003).
[3] J. Huh, V. V. Ginzburg, and A. C. Balazs, Macromolecules **33**, 8085 (2000).
[4] A. J. Schultz, C. K. Hall, and J. Genzer, Macromolecules **38**, 3007 (2005).
[5] A. C. Balazs, V. V. Ginzburg, F. Qiu, G. Peng, and D. Jasnow, J. Phys. Chem. B **104**, 3411 (2000).
[6] V. V. Ginzburg, C. Gibbons, F. Qiu, G. Peng, and A. C. Balazs, Macromolecules **33**, 6140 (2000).
[7] K. F. Freed, Adv. Chem. Phys. **22**, 1 (1972).
[8] K. M. Hong and J. Noolandi, Macromolecules **14**, 727 (1981).
[9] M. W. Matsen, J. Phys. Condens. Matter **14**, R21 (2002).
[10] M. W. Matsen and M. Schick, Phys. Rev. Lett. **72**, 2660 (1994).
[11] N. Maurits and J. G. E. M. Fraaije, J. Chem. Phys. **107**, 5879 (1997).
[12] F. Drolet and G. H. Fredrickson, Phys. Rev. Lett. **83**, 4317 (1999).
[13] G. H. Fredrickson, V. Ganesan, and F. Drolet, Macromolecules **35**, 16 (2002).
[14] G. A. Buxton, J. Y. Lee, and A. C. Balazs, Macromolecules **36**, 9631 (2003).
[15] R. B. Thompson, V. V. Ginzburg, M. W. Matsen, and A. C. Balazs, Macromolecules **35**, 1060 (2002).
[16] J. Y. Lee, Z. Shou, and A. C. Balazs, Phys. Rev. Lett. **91**, 136103 (2003).
[17] R. Car and M. Parrinello, Phys. Rev. Lett. **55**, 2471 (1985).
[18] M. Doi and S. Edwards, *The Theory of Polymer Dynamics* (Clarendon Press, Oxford, 1986).
[19] G. Tzeremes, K. O. Rasmussen, T. Lookman, and A. Saxena, Phys. Rev. E **65**, 041806 (2002).
[20] V. Ganesan and G. H. Fredrickson, Europhys. Lett. **55**, 814 (2001).
[21] G. Parisi, Phys. Lett. **131B**, 393 (1983).
[22] S. W. Sides and G. H. Fredrickson, Polymer **44**, 5859 (2003).
[23] D. L. Ermak, J. Chem. Phys. **62**, 4189 (1975).
[24] B. J. Kim, J. J. Chiu, G. Yi, D. J. Pine, and E. J. Kramer, Adv. Mater. **17**, 2618 (2005).
[25] M. Brust, M. Walker, D. Bethell, D. Schiffrin, and R. Whyman, J. Chem. Soc. Chem. Commun. **xx**, 801 (1994).
[26] B. J. Kim, J. Bang, C. J. Hawker, and E. J. Kramer, Macromolecules (to be published).